Dissociative attachment and vibrational excitation in low-energy collisions of electrons with H_2 and D_2

J. N. Bardsley and J. M. Wadehra
Physics Department, University of Pittsburgh, Pittsburgh, Pennsylvania 15260
(Received 27 April 1979)

A semiempirical analysis is made of the contributions of the two lowest resonant states to dissociative attachment and vibrational excitation in low-energy collisions of electrons with H_2 and D_2. The resonance models are based both on *ab initio* calculations and on fits to experimental data. The dissociative-attachment cross section near threshold is enhanced significantly by vibrational or rotational excitation of the initial molecule. Near 10 eV, contributions from both resonances are required to explain the observed cross sections for vibrational excitation.

I. INTRODUCTION

The study of collisions of slow electrons with H_2, D_2, and N_2 has provided quantitative tests of the resonance theories of electron-molecule scattering.[1-7] Dubé and Herzenberg[8] have recently made a comparison between theory and experiment concerning the absolute values of the cross sections for inelastic e-N_2 collisions at low energies. The recent experimental studies of dissociative attachment[9] and vibrational excitation[10] in electron collisions with H_2 and D_2 and the renewed interest in negative ion production in hydrogen plasmas[11,12] have demonstrated the need for further theoretical study on these molecules. In this paper we report calculations of the contributions of the two lowest resonant states of H_2^- and D_2^- to vibrational excitation and dissociative attachment at energies below 12 eV.

This work has three specific aims. The first is to explore the dependence of the cross section for dissociative attachment near threshold upon the vibrational and rotational state of the initial H_2 molecule. The second is to answer a question posed by Fiquet-Fayard,[13] whether the rapid decrease in the dissociative attachment cross section above its threshold near 3.75 eV and the very slow decrease in the vibrational excitation cross sections $\sigma_{0,1}$ and $\sigma_{0,2}$ can be explained in terms of resonant scattering alone. The third aim is to analyze the recent measurements by Hall[10] of vibrational excitation cross sections near 10 eV. The ratios $\sigma_{0,v+1}/\sigma_{0,v}$ are of the order of 0.1 for small v but close to 1 for large v.

II. RESONANT SCATTERING MODEL

We will use the traditional resonant scattering theory[4,7] with a local width, which gives vibrational excitation cross sections that vanish at threshold and elastic cross sections that do not violate unitarity very seriously for very large resonance widths.[14] During the lifetime of the resonant state of the negative ion, the radial nuclear wave function $\xi_J(R)$ satisfies the equation

$$\left(-\frac{1}{2M}\frac{d^2}{dR^2}+\frac{J(J+1)}{2MR^2}+V^-(R)-\frac{i}{2}\Gamma(R)-E\right)\xi_J(R)$$
$$=\zeta_{vJ}(R)[\Gamma_0(R)/2\pi k_0(R)]^{1/2}, \quad (1)$$

in which M is the reduced mass of the nuclei, J and E give the total angular momentum and energy, $V^-(R)$ and $\Gamma(R)$ are the potential energy and width for the appropriate electronic state of the negative ion, and $\zeta_{vJ}(R)$ is the radial nuclear wave function corresponding to the initial vibrational and rotational state of the neutral molecule. The function $k_0(R)$ gives the wave number of the electrons that can be captured when the nuclei are at the separation R without a change in the nuclear velocity. It is defined in terms of the potential-energy curve $V_0(R)$ for the ground state of H_2 by

$$\tfrac{1}{2}k_0^2(R)=V^-(R)-V_0(R). \quad (2)$$

$\Gamma_0(R)$ is the partial width for decay to the ground electronic state of H_2.

The boundary conditions imposed on Eq. (1) are

$$\xi_J(R)=0 \text{ for } R=0$$

and

$$\frac{d\xi_J}{dR}=iK_0(R)\xi_J \text{ as } R\to\infty,$$

where

$$K_0^2(R)=2M\lim_{R\to\infty}[E-V^-(R)].$$

In constructing Eq. (1) we have neglected the change in the angular momentum of the nuclei due to the capture of the third electron. This effect was included in our earliest calculations, but its effect is very small, unless one wishes to study

angular distributions.

The cross section for dissociative attachment can be obtained from the asymptotic behavior of $\xi_J(R)$ through

$$\sigma_{DA}=\frac{2\pi^2}{k}\frac{K}{M}\lim_{R\to\infty}|\xi_J(R)|^2, \tag{3}$$

where k and K are the wave numbers describing the incident electronic motion and the outgoing ion motion in the center-of-mass frame. The vibrational excitation cross sections are best described in terms of the Green's function $G(R,R')$ appropriate to the operator on the left-hand side of Eq. (1) as

$$\sigma_{vv'}=\pi\frac{k'}{k}\left|\int\int dRdR'\zeta^*_{v'}(R')\left(\frac{\Gamma_0(R')}{k_0(R')}\right)^{1/2}\times G(R',R)\left(\frac{\Gamma_0(R)}{k_0(R)}\right)^{1/2}\zeta_v(R)\right|^2, \tag{4}$$

in which k' is the wave number describing outgoing electronic motion. The principle of detailed balancing, evidently guaranteed by the above expression for the vibrational excitation cross section, also provides a useful numerical check on calculations.

For scattering below 11 eV we need to consider the $X^2\Sigma_u^+(1\sigma_g)^2(1\sigma_u)$ and $B^2\Sigma_g^+(1\sigma_g)(1\sigma_u)^2$ resonant states of H_2^-. For the $X^2\Sigma_u^+$ state electron emission can lead only to the ground electronic state of H_2, so that $\Gamma(R)=\Gamma_0(R)$. For this state the potential $V^-(R)$ was parametrized in the form

$$V^-(R)=V_u^-(R)=V_0(R)-A+0.2152\exp(-0.2276R^2)\text{a.u.}$$

The constant A was set equal to the affinity of H (0.022 71 a.u.) and the other numerical constants were chosen so that the H_2^- curve is approximately 3 eV above that of H_2 at the equilibrium separation (1.4 a_0) and crosses the H_2 curve at 3.0 a_0, consistent with the *ab initio* calculations of Bardsley *et al.*[4] The width $\Gamma(R)$ was taken to be

$$\Gamma(R)=\Gamma_u(R)=Ck_u^3(R)$$

reflecting the p-wave natures of this resonance; $k_u(R)$ is as defined by Eq. (2) with $V^-(R)=V_u^-(R)$. The constant C was chosen to give agreement with the observed cross section for dissociative attachment at 3.75 eV. The relative cross sections for dissociative attachment in H_2, HD, and D_2 between 3.75 and 15 eV were measured by Schulz and Asundi.[15] By normalizing to absolute cross sections for H_2 near 14 eV obtained by Rapp *et al.*[16] or by Schulz,[17] the H_2 cross section at 3.75 eV was deduced to be either 1.6×10^{-21} cm^2 or 2.8×10^{-21} cm^2. The values of C required to reproduce these values are (in atomic units) 2.966 and 2.65, respectively. In calculations that have already been reported[18] the choice between these two values was based on an analysis of the isotope effect. The ratio of the threshold attachment cross sections for H_2 and D_2 was calculated to be about 540 with $C=2.966$ and 410 with $C=2.65$. The measured ratio of ~200 was taken as support for the smaller value of C. However the theoretical values for the cross section ratio between H_2 and HD are 10.5 for $C=2.966$ and 9.5 for $C=2.65$. The experimental value of ~16 supports the higher value for C corresponding to the value of 1.6×10^{-21} cm^2 for the threshold attachment cross section of H_2. In this paper we use the higher value of C throughout.

This discussion shows that there appears to be an inconsistency between our calculations and the isotope effect measurements of Schulz and Asundi.[15] The cross sections for D_2 are so small that we believe further experimental study would be worthwhile. In the meantime we feel greater confidence in using the $\sigma_{HD}:\sigma_{H_2}$ ratio to guide our choice of C.

The $^2\Sigma_g^+$ resonance can decay into both the $X^1\Sigma_g^+$ state and $^3\Sigma_u^+$ states of H_2, so that we must specify two partial widths $\Gamma_{g0}(R)$ and $\Gamma_{g1}(R)$. The potential curve of this resonance is related to the potential curve $V_1(R)$ for the repulsive $b^3\Sigma_u^+$ state of H_2 through

$$V^-(R)=V_g^-(R)=V_1(R)-A+0.0332\exp(-0.0069R^2)\text{ a.u.}$$

Ab initio calculations suggest that the repulsive H_2^- and H_2 potential curves cross near 5.1 a_0,[19] and the shape of the dissociative attachment cross section suggests that the two curves remain close together at smaller R. These conditions guided our choice of numerical constants in $V_g^-(R)$. The partial decay widths are taken to be (in atomic units)

$$\Gamma_{g0}(R)=0.005k_{g0}(R),$$

$$\Gamma_{g1}(R)=56.0k_{g1}^3(R),$$

in which

$$\tfrac{1}{2}k_{gi}^2(R)=V_g^-(R)-V_i(R)\quad(i=0,1).$$

The numerical constants in the widths were chosen so as to fit the experimental dissociative attachment cross section for H_2 near 10 eV and give approximate agreement with respect to the excitation of high vibrational levels.

Potential curves for the $X^1\Sigma_g^+$ and $b^3\Sigma_u^+$ states of the neutral molecule were taken from the standard work of Kolos and Wolniewicz.[20] An eight-point Lagrange interpolation routine[21] was used to interpolate between the published values on the curves. At large internuclear separations the curves were

fitted to the appropriate asymptotic form. Equation (1) was solved numerically both through the direct solution of the inhomogeneous equation and through the construction of the Green's function. The wave function $\xi_J(R)$ was obtained between $R = 0.4a_0$ and $15.0a_0$ in steps of $0.0125a_0$ using the Numerov technique. Simpson's rule was used for integration over the Green's function. After checking the two procedures for consistency, the Green's-function procedure was used for final results. The computer program was checked by comparison with the results of Dubé and Herzenberg on vibrational excitation in N_2.

Another check on the numerical accuracy is provided by the equation

$$\frac{K_0}{M}\lim_{R\to\infty}|\xi_J|^2+\int_0^\infty \Gamma(R)|\xi_J|^2 dR$$

$$=2\int_0^\infty \zeta_{vJ}(R)\left(\frac{\Gamma_0(R)}{2\pi k_0(R)}\right)^{1/2}\mathrm{Im}\xi_J(R)\,dR\,,$$

which is obtained by multiplying Eq. (1) by ξ_J^*, subtracting its complex conjugate, and integrating.

The potential curves for the $X^1\Sigma_g^+$ and $b^3\Sigma_u^+$ states of the neutral molecule and for the real parts of the $^2\Sigma_u^+$ and $^2\Sigma_g^+$ state of the negative molecular ion are shown in Fig. 1. Asymptotically, both $^1\Sigma_g^+$ and $^3\Sigma_u^+$ states go over into two separated atoms in the ground state, and both $^2\Sigma_u^+$ and $^2\Sigma_g^+$ go over into an atom in the ground state and a negative atomic ion in the ^1S state. The $^2\Sigma_g^+$ state lies so close to the $^3\Sigma_u^+$ state that the curves are almost indistinguishable in Fig. 1. The imaginary parts of the negative molecular ion potential are shown in Fig. 2.

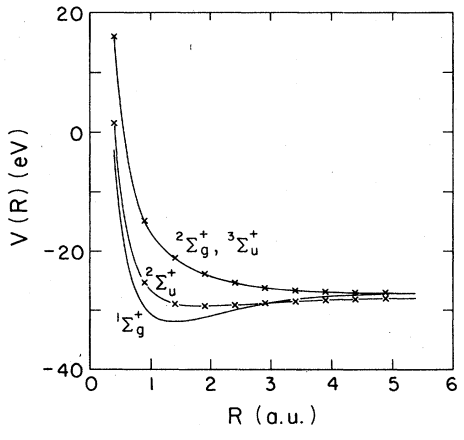

FIG. 1. Potential-energy curves for the real parts of the $^2\Sigma_g^+$ and $^2\Sigma_u^+$ resonant states of the negative molecular ion and for the $^1\Sigma_g^+$ and $^3\Sigma_u^+$ states of the neutral molecule.

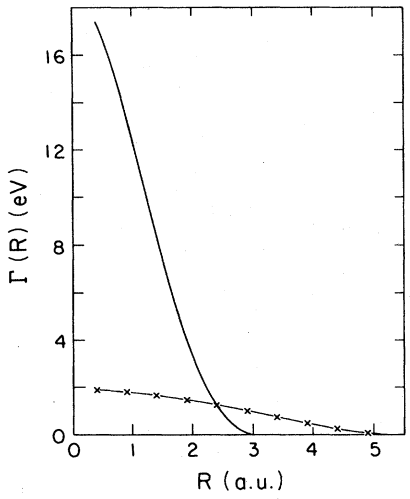

FIG. 2. Imaginary parts of the resonant molecular-ion potential; Solid line, $^2\Sigma_u^+$; line with crosses, $^2\Sigma_g^+$.

III. RESULTS AND DISCUSSION

Figures 3 and 4 show the dissociative attachment cross sections for D_2 near threshold, for various vibrational and rotational states of the D_2 molecule. In both cases the enhanced cross sections associated with excited states arise from an increase in the survival factor, which is the probability that the D_2^- dissociates without emitting an electron. This factor is increased because capture can occur at larger values of R due to the larger ampli-

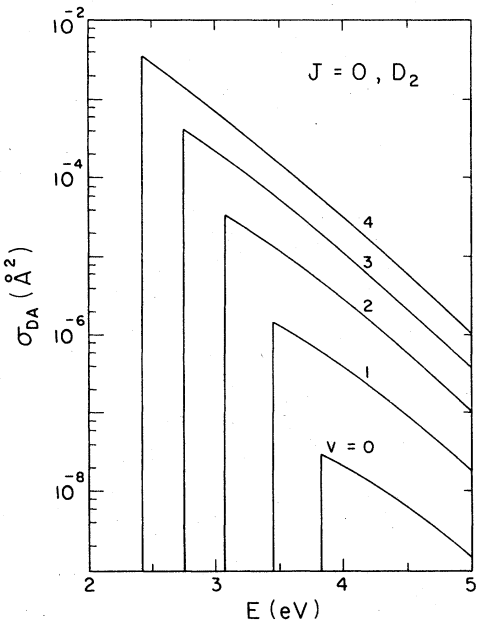

FIG. 3. Dissociative-attachment cross sections for various rotationless vibrational states of D_2.

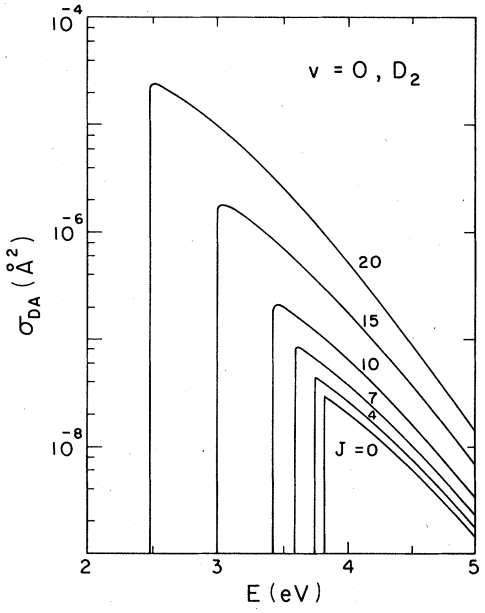

FIG. 4. Dissociative-attachment cross sections for various rotational levels of the ground vibrational state of D_2.

tude of the vibrational motion in excited states, and the centrifugal stretching in excited rotational levels. We believe that the change in the survival factor is much more important than changes in the Franck-Condon factors in the capture cross section. We did not deem it necessary to give corresponding results for H_2, since in our previous work[18] we presented (with a slightly different normalization, as explained above) in detail the vibrational and rotational state dependence of attachment cross sections in e-H_2 collisions.

Table I gives the attachment cross sections near thresholds for several rotational and vibrational states of both H_2 and D_2. In Fig. 5 the cross-section ratios are compared with the experimental results of Allan and Wong[9] and with our earlier calculations. The new calculations give slightly better agreement with experiment for excited vibrational levels of H_2 and D_2 but are not significantly better in other respects.

The effect of rotational excitation seen in our calculation and the experimental results of Allan and Wong[9] is intermediate between the earlier experiments of Spence and Schulz,[22] which gave no clear evidence of enhancement, and the calculations of Chen and Peacher,[6] which predicted a much larger effect. Since our resonance model is similar to that of Chen and Peacher, the reason for the difference between the two theoretical results is unclear. For D_2 the rotational spacings are so small that even at 300K the observed cross sections do not give directly an accurate value for attachment to the ground state. However, the effects of rotational excitation in D_2 at 300K are not large enough to explain the discrepancy concerning the isotope ratios discussed above.

Figures 6 and 7 show the contributions of the two resonances to vibrational excitation between 2 and 12 eV for H_2 and D_2, respectively. It is clear from a comparison of Figs. 3 and 7 that the disparate rate of decrease of the dissociative attachment and vibrational excitation cross sections is reproduced, at least qualitatively, by the resonance theory. This behavior indicates that the rapid decrease in σ_{DA} is due primarily to the energy dependence of the survival factor rather than the Franck-Condon overlaps.

It is clear from Figs. 6 and 7 that near 10-eV vibrational excitation cross sections $\sigma_{0,1}$ and $\sigma_{0,2}$ are dominated by the lower $^2\Sigma_u^+$ resonance, whereas excitation of the higher levels proceeds predominantly through the $^2\Sigma_g^+$ resonance. This explains the change in the ratios $\sigma_{0,v+1}/\sigma_{0,v}$ mentioned in the Introduction. One would also expect to find different angular distributions associated with the excitation of low and high vibrational levels. Our results are consistent with the observation by Hall[10] of a peak near 10 eV in $\sigma_{0,3}$ for D_2 and the monotonic decrease of $\sigma_{0,1}$ for H_2 found by Ehrhardt

TABLE I. Attachment cross sections near threshold for various vibrational-rotational levels of H_2 and D_2.

v	J	E(eV)	σ_{DA}(cm^2) H_2	E(eV)	σ_{DA}(cm^2) D_2
0	0	3.73	1.6(−21)	3.83	3.0(−24)
0	1	3.73	1.7(−21)	3.80	3.3(−24)
0	2	3.70	1.9(−21)	3.80	3.4(−24)
0	3	3.65	2.3(−21)	3.78	3.9(−24)
0	4	3.60	2.8(−21)	3.75	4.5(−24)
0	5	3.53	3.7(−21)	3.70	5.7(−24)
0	6	3.45	5.0(−21)	3.68	6.8(−24)
0	7	3.35	7.2(−21)	3.63	8.8(−24)
0	8	3.25	1.1(−20)	3.58	1.2(−23)
0	10	3.13	2.2(−20)	3.43	2.2(−23)
0	15	2.38	3.2(−19)	3.03	2.0(−22)
0	20	1.63	5.5(−18)	2.55	2.5(−21)
1	0	3.23	5.5(−20)	3.45	1.5(−22)
2	0	2.73	8.0(−19)	3.08	3.3(−21)
3	0	2.28	6.3(−18)	2.75	4.2(−20)
4	0	1.85	3.2(−17)	2.43	3.6(−19)
5	0	1.45	1.1(−16)	2.10	2.2(−18)
6	0	1.08	3.0(−16)	1.80	1.0(−17)
7	0	0.73	4.5(−16)	1.53	3.3(−17)
8	0	0.40	3.5(−16)	1.25	9.6(−17)
9	0	0.13	4.8(−16)	1.00	2.3(−16)
10	0			0.75	4.1(−16)
11	0			0.53	3.8(−16)
12	0			0.30	3.7(−16)
13	0			0.10	4.6(−16)

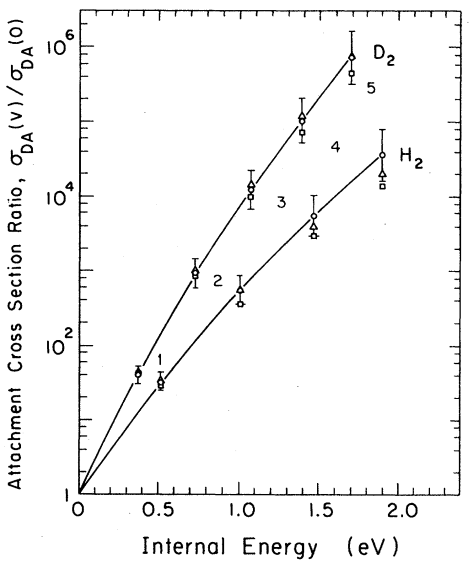

FIG. 5. Internal-state dependence of threshold dissociative attachment cross sections in H_2 and D_2 via $^2\Sigma_u^+$ resonance; circles, experiment (Ref. 9); squares, previous theoretical results (Ref. 18); triangles, present results.

et al.[23] This change in the relative importance of the two resonances arises because the $^2\Sigma_u^+$ resonance has a large entry width and a very short lifetime against electron emission. The $^2\Sigma_g^+$ resonance has a very small entry width and a slightly longer lifetime against autodetachment. Thus although electron capture into the $^2\Sigma_g^+$ resonance is more difficult, its formation will lead to a greater transfer of kinetic energy to the nuclei, producing

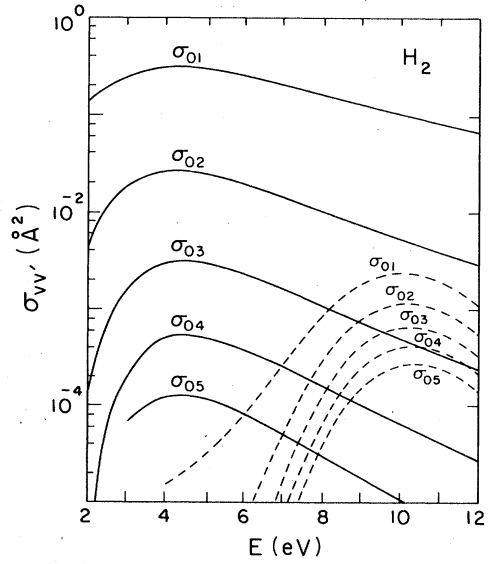

FIG. 6. Contributions of the two lowest resonant states to the vibrational excitation cross sections of H_2; solid lines, $^2\Sigma_u^+$; dashed lines, $^2\Sigma_g^+$.

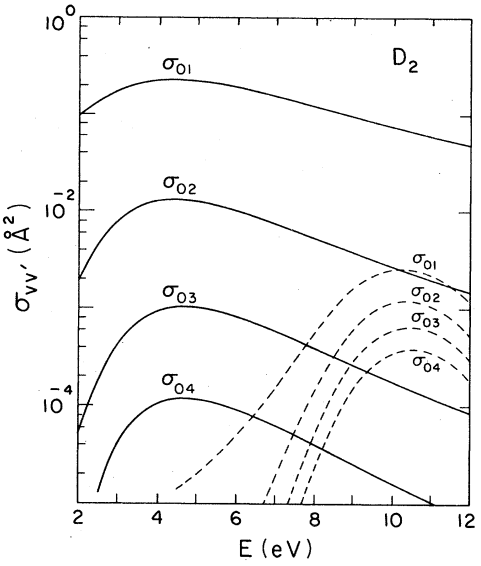

FIG. 7. Contributions of the two lowest resonant states to the vibrational excitation cross sections of D_2; solid lines, $^2\Sigma_u^+$; dashed lines, $^2\Sigma_g^+$.

relatively large cross sections for the excitation of high vibrational levels and dissociative attachment.

One feature of the experimental data noted by Hall[10] is that the peak in the vibrational excitation cross section $\sigma_{0,3}$ in D_2 near 10 eV occurs approximately 0.5 eV below the corresponding peak in σ_{DA}. This is also seen in our cross sections, but the rapid decrease in $\sigma_{0,3}$ observed between 10 and 11 eV is not reproduced well in our results. Clearly the observed structure between 11.3 and 12 eV due to higher resonances is not apparent in these calculations.

In Fig. 8 we show the ratio of vibrational excitation to elastic cross sections, $\rho(v)=\sigma_{0,v}/\sigma_{0,0}$, as a function of excitation energy for incident electron energy of 10 eV. The cross section $\sigma_{0,0}$ used as a normalization factor is calculated from the resonance model, and therefore does not include the direct nonresonant contribution. The cross section for excitation to a level v is predicted,[24] in the impulse limit, to be proportional to $M^{-v/2}$, where M is the reduced mass. Thus the cross section for D_2 multiplied by $2^{v/2}$ should reproduce the H_2 cross sections. The dashed curve in Fig. 8 indicates that this isotopic behavior overestimates the H_2 cross sections for large v but reproduces the H_2 cross sections quite well for small v. This can be understood within our model, since for small v the excitation cross section is dominated by the $^2\Sigma_u^+$ resonance, which is quite broad in width and is basically an "impulse" resonance. For large v, on the other hand, significant contribution to the

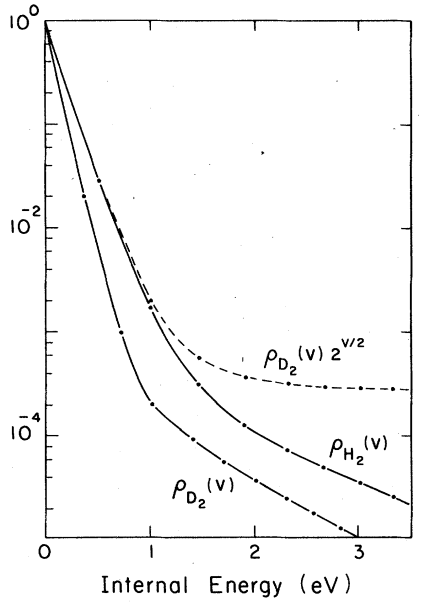

FIG. 8. Internal-state dependence of the ratio of vibrational excitation to elastic cross sections, $\rho(v) = \sigma_{0,v}/\sigma_{0,0}$, for incident electron energy of 10 eV.

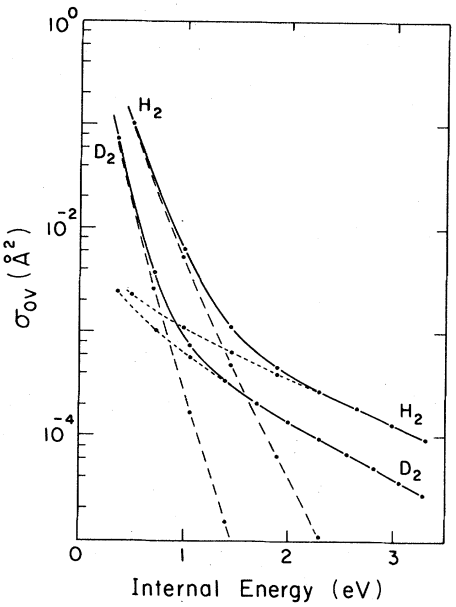

FIG. 9. Internal-state dependence of the contributions of the two lowest resonant states to the vibrational-excitation cross sections for incident electron energy of 10 eV; long-dash lines, $^2\Sigma_u^+$; short-dash lines $^2\Sigma_g^+$; solid lines, total contribution of the two resonances.

excitation cross sections comes from the $^2\Sigma_g^+$ resonance, which is relatively narrow. The absolute contributions of the two resonances to the vibrational excitation cross sections are shown in Fig. 9, as a function of energy loss, for incident electron energy of 10 eV.

Finally, superelastic, elastic, and inelastic cross sections for incident electron energies of 6 and 8 eV are given in Tables II and III.

IV. CONCLUSIONS

In spite of the very large widths of the two lowest resonant states of H_2^- and D_2^-, the theory successfully reproduces the qualitative features of the experimental data below 11 eV, and explains the different shapes among the cross sections for vibrational excitation and dissociative attachment. However there appears to be significant difference between theory and experiment concerning the magnitude of the isotope effect in dissociative attachment. The theory has provided estimates of the dissociative attachment cross sections from excited states of H_2. These results are consistent with the threshold cross sections observed by Allan and Wong.[9]

TABLE II. The vibrational-excitation cross sections (in Å^2) of H_2 (upper entry) and D_2 (lower entry) for electron energy of 6 eV. v and v' are the initial and the final vibrational state of the molecule, respectively.

v / v'	0	1	2	3	4	5
0	9.5	2.6(−1)	1.7(−2)	1.8(−3)	3.0(−4)	1.2(−4)
	9.8	1.9(−1)	9.2(−3)	6.8(−4)	6.8(−5)	1.4(−5)
1	2.6(−1)	7.6	4.6(−1)	4.6(−2)	6.9(−3)	1.5(−3)
	1.9(−1)	8.4	3.5(−1)	2.6(−2)	2.7(−3)	4.0(−4)
2	2.0(−2)	4.8(−1)	5.9	6.1(−1)	8.0(−2)	1.5(−2)
	1.0(−2)	3.6(−1)	7.1	4.9(−1)	4.8(−2)	6.6(−3)
3	2.4(−3)	5.5(−2)	6.2(−1)	4.5	6.9(−1)	1.1(−1)
	8.3(−4)	2.9(−2)	5.0(−1)	5.9	5.9(−1)	7.2(−2)
4	3.9(−4)	9.2(−3)	9.3(−2)	7.1(−1)	3.4	7.4(−1)
	9.1(−5)	3.4(−3)	5.4(−2)	6.0(−1)	4.9	6.6(−1)
5	8.3(−5)	1.9(−3)	2.0(−2)	1.3(−1)	7.5(−1)	2.6
	1.3(−5)	4.7(−4)	8.0(−3)	8.1(−2)	6.7(−1)	4.1

TABLE III. The vibrational-excitation cross sections (in Å^2) of H_2 (upper entry) and D_2 (lower entry) for electron energy of 8 eV. v and v' are the initial and the final vibrational state of the molecule, respectively.

v' \ v	0	1	2	3	4	5
0	5.9	1.6(−1)	9.2(−3)	1.4(−3)	5.0(−4)	3.7(−4)
	6.1	1.2(−1)	5.0(−3)	6.3(−4)	3.0(−4)	2.3(−4)
1	1.7(−1)	4.7	2.9(−1)	2.3(−2)	3.0(−3)	5.7(−4)
	1.2(−1)	5.2	2.2(−1)	1.4(−2)	1.7(−3)	4.0(−4)
2	1.1(−2)	3.0(−1)	3.7	3.8(−1)	4.1(−2)	6.6(−3)
	5.4(−3)	2.3(−1)	4.4	3.0(−1)	2.4(−2)	3.0(−3)
3	1.2(−3)	2.9(−2)	4.0(−1)	2.9	4.5(−1)	5.9(−2)
	4.4(−4)	1.6(−2)	3.1(−1)	3.7	3.7(−1)	3.6(−2)
4	2.3(−4)	4.6(−3)	4.8(−2)	4.6(−1)	2.2	4.9(−1)
	6.2(−5)	1.9(−3)	2.8(−2)	3.8(−1)	3.1	4.2(−1)
5	6.9(−5)	1.1(−3)	9.1(−3)	6.8(−2)	5.0(−1)	1.7
	1.7(−5)	4.0(−4)	3.9(−3)	4.1(−2)	4.3(−1)	2.6

The large enhancement in dissociative attachment to H_2 might explain the anomalously high densities of H^- ions seen in a dilute hydrogen plasma by Nicolopoulou *et al.*[11] However, calculations of the populations of the excited H_2 states in their plasma are required before any conclusions can be reached.

Our calculations support the *ab initio* calculations[4,19,25] that show that the excited $B^2\Sigma_g^+$ state of H_2^- can decay into the $b^3\Sigma_u$ state of H_2 over a wide range of internuclear separations. This suggests that dissociative excitation

$$e + H_2 \rightarrow H + H + e$$

should take place around 10 eV with a cross section of the order of 10^{-17} cm^2. An absolute measurement of this cross section would be valuable.

The experimental data concerning absolute cross sections for low-energy e-H_2 collisions is fragmentary, and some of the most important information was obtained many years ago. There is a need for a comprehensive study of the cross sections for vibrational, electronic, and dissociative excitation and dissociative attachment below, say, 20 eV. A parallel theoretical effort would help us to assess further the accuracy of resonant scattering, and would be beneficial in filling in the gaps in data accumulation that are currently inaccessible to experiment.

ACKNOWLEDGMENTS

This work was supported by the National Science Foundation through Grant No. 76-21456. The authors are grateful to L. Dubé, A. Herzenberg, R. I. Hall, M. Allan, and S. F. Wong for communicating their results in advance of publication, to M. Bacal for demonstrating the need for further study of dissociative attachment, and to the Theoretical Division of the Los Alamos Scientific Laboratory for provision of computer time.

[1]A. Herzenberg and F.Mandl, Proc. Roy. Soc. London Sect. A 270, 48 (1962).
[2]J. C. Y. Chen, J. Chem. Phys. 40, 3507 (1964); 40, 3513 (1964).
[3]Yu. N. Demkov, Phys. Lett. 15, 235 (1965).
[4]J. N. Bardsley, A. Herzenberg, and F. Mandl, Proc. Phys. Soc. London 89, 305 (1966); 89, 321 (1966).
[5]T. F. O'Malley, Phys. Rev. 150, 14 (1966); 156, 230 (1967).
[6]J. C. Y. Chen and J. L. Peacher, Phys. Rev. 163, 103 (1967).
[7]D. T. Birtwistle and A. Herzenberg, J. Phys. B 4, 53 (1970).
[8]L. Dubé and A. Herzenberg, Phys. Rev. A 20, 194 (1979).
[9]M. Allan and S. F. Wong, Phys. Rev. Lett. 41, 1791 (1978).
[10]R. Hall, in *Invited Papers and Progress Reports, ICPEAC X* (North-Holland, Amsterdam, 1978), p. 25.
[11]E. Nicolopoulou, M. Bacal, and H. J. Doucet, J. Phys. (Paris) 38, 1399 (1977).
[12]M. Bacal and G. W. Hamilton, Phys. Rev. Lett. 42, 1538 (1979).
[13]F. Fiquet-Fayard, Vacuum 24, 533 (1974).
[14]J. N. Bardsley, in *Electron-Molecule and Photon-Molecule Collisions*, edited by T. Rescigno, V. McKoy, and B. Schneider (Plenum, New York, 1979), p. 267.
[15]G. J. Schulz and R. K. Asundi, Phys. Rev. 188, 280 (1966).
[16]D. Rapp, T. E. Sharp, and D. D. Briglia, Phys. Rev. Lett. 14, 533 (1965).
[17]G. J. Schulz, Phys. Rev. 113, 816 (1959).
[18]J. M. Wadehra and J. N. Bardsley, Phys. Rev. Lett. 41, 1795 (1978).

[19]J. N. Bardsley and J. S. Cohen, J. Phys. B 11, 3645 (1978).
[20]W. Kolos and L. Wolniewicz, J. Chem. Phys. 43, 2429 (1965).
[21]*Handbook of Mathematical Functions*, edited by M. Abramowitz and I. A. Stegun [Natl. Bur. Stand. (U.S.), GPO, Washington, D.C., 1964].
[22]D. Spence and G. J. Schulz, Phys. Rev. 188, 280 (1969).
[23]H. Ehrhardt, L. Laughans, F. Linder, and H. S. Taylor, Phys. Rev. 173, 222 (1968).
[24]E. S. Chang and S. F. Wong, Phys. Rev. Lett. 38, 1327 (1977).
[25]B. D. Buckley and C. Bottcher, J. Phys. B 10, L635 (1977).